Supplementary Material

Enhanced ethene to propene ratio over Zn modified SAPO-34 zeolites in methanol-to-olefin reaction

Huiwen Huang Haoren Wang Hui Zhu Shanhe Zhang Qiang Zhang Chunyi Li*

State Key Laboratory of Heavy Oil Processing, China University of Petroleum (East China), Qingdao 266580, China

***Corresponding Author:** chyli_upc@126.com (C. Li)

S1. Experimental

S1.1. Catalyst preparation

SAPO-34 (SiO_2/Al_2O_3 = 0.4, P_2O_5/Al_2O_3 = 1.0) zeolite in its templated form was purchased from Catalyst Plant of Nankai University, and the sample was calcined at 600 °C for 4 h in a muffle furnace to achieve H-SAPO-34. The NH_4-SAPO-34 was obtained by three consecutive ion-exchanges of H-SAPO-34 with 1 M NH_4NO_3 solution at 80 °C for 2 h, which was followed by filtration, washing and drying. The Zn-modified SAPO-34 zeolites were prepared by the impregnation method. The NH_4-SAPO-34 was stirred in a certain concentration of $Zn(NO_3)_2 \cdot 6H_2O$ solution with liquid-to-solid ratio of 30 mL/g at room temperature for 4 h, dried at 120 °C overnight and calcined at 600 °C for 3 h in a muffle furnace. The obtained SAPO-34 zeolites with Zn modification is denoted as *x*Zn/SAPO-34, where *x* represents the mass percentage of Zn on the catalyst (*x* = 0.5, 1.0, 2.0, 6.0 and 9.0). Prior to catalytic tests, all sample powders were pressed into wafers, and subsequently crushed and sieved into 40-60 mesh particles.

S1.2. Catalyst characterization

X-ray diffraction (XRD) patterns were obtained on an X'Pert PRO MPD diffractometer (PANalytical Co., Netherlands) with monochromatic Cu Kα radiation (40 kV and 40 mA) in the 2θ range from 5° to 65° at a scanning speed of 2 °/min.

Scanning electron microscope (SEM) images were examined by an S-4800 field emission scanning electron microscope (Hitachi Co., Japan) with an acceleration voltage of 3 kV.

Nitrogen adsorption-desorption isotherms were measured on a Quadrasorb SI apparatus (Quantachrome, USA) at liquid nitrogen temperature. Prior to the measurement, the zeolite sample was evacuated at 300 °C for 6 h to remove the adsorbed moisture. The total BET surface area was calculated by the Brunauer-Emmett-Teller (BET) equation and the total pore volume was estimated from the nitrogen (N_2) adsorbed volume at relative pressure of 0.99. The micropore surface area and micropore volume were determined by the *t*-plot method. The external surface area and mesopore volume were the difference between the total calculated value and the corresponding micropore data.

Temperature-programmed desorption of ammonia (NH_3-TPD) was performed on a PCA-1200 chemisorption analyzer (Biaode Electronic Technology Co., China) with an on-line thermal conductivity detector (TCD). Firstly, about 100 mg sample of 40-60 mesh was loaded into a U-shaped micro-reactor and pretreated at 600 °C for 30 min with flowing argon (50 mL/min), and then cooled down to 100 °C and saturated with NH_3. Secondly, the sample was purged with helium (30 mL/min) to remove the physically adsorbed NH_3 until a stable TPD signal was attained. Finally, the temperature was increased from 100 to 600 °C at a constant heating rate of 10 °C/min.

Temperature-programmed reduction by hydrogen (H_2-TPR) was carried out on a PCA-1200 chemisorption analyzer (Biaode Electronic Technology Co., China) with an on-line TCD. About 200 mg

sample of 40-60 mesh was loaded into a U-shaped micro-reactor and pretreated at 500 °C for 30 min with flowing argon (50 mL/min). After cooling down to room temperature, the gas was switched to 5 vol% H_2/N_2 (30 mL/min), and the temperature was raised from room temperature to 800 °C at a constant heating rate of 10 °C/min as the TCD signal got stable.

Fourier-transform infrared spectroscopy (FTIR) measurements were conducted on a Tensor 27 FTIR instrument (Bruker, USA) equipped with a MCT detector at the resolution of 4 cm^{-1} and 64 scans. Prior to the measurement, the zeolite sample was pressed into a wafer and placed in an evacuable Pyrex glass cell equipped with CaF_2 windows. Afterward, the self-supported wafer was pretreated in situ at 500 °C and 1.0×10^{-3} kPa for 30 min to remove the adsorbed water, and then cooled to 30 °C, and the FTIR spectrum was recorded in the range of 4000-400 cm^{-1}. The spectrum of KBr under the same condition was used as the background.

Diffuse reflectance ultraviolet-visible spectra (UV-vis DRS) were recorded on a Varian Cary 300 Scan UV-vis spectrophotometer equipped with an integration sphere at room temperature. The spectra were recorded under air-exposed conditions in the range of 500-200 nm.

Thermo-gravimetric analysis (TGA) was performed on a DTU-2A differential thermogravimetric analyzer. The sample was heated from 20 °C to 800 °C at a heating rate of 10 °C /min under flowing air (60 mL/min). The amount of the deposited coke on the catalyst after MTO reaction is determined from the weight loss occurring at 400-700 °C from TGA curves.

S1.3. Catalytic test

MTO reactions were carried out in a fixed-bed tubular stainless steel micro-reactor (10 mm inner diameter) at 500 °C under atmospheric pressure. The reactor was heated by a resistive furnace and the temperature was measured by an internal thermocouple, which was positioned in the center of the catalyst

bed. For each test, 1.0 g zeolite of 40-60 mesh was loaded into the center of the reactor, and the volume up- and down-flow to the catalyst bed was respectively filled with 1 mL inert quartz sands to prevent temperature profile along the catalyst bed. Prior to the catalytic test, the zeolite was activated at 550 °C in flowing nitrogen (20 mL/min) for 30 min and cooled down to the reaction temperature. Then, liquid methanol with weight hourly space velocity of 10.02 h^{-1} was fed through a HPLC infusion pump into the reactor with flowing nitrogen (20 mL/min) as carrier gas. The reactor exit stream was separated into gaseous phases and aqueous phases by a cold trap. The gaseous phases were analyzed by a Bruker 450 gas chromatography (GC) equipped with a flame ionization detector (FID) and two TCDs, and the aqueous phases were analyzed on an Agilent 6820-GC fitted with HP-INNOWAX capillary column (30 m × 0.32 mm × 0.25 μm) and a FID, using ethanol as the internal standard for calibration.

The activity of the zeolite samples is expressed in terms of methanol conversion, which is calculated from the difference between the inlet and outlet concentrations of methanol and dimethyl ether (DME). Product selectivity on a carbon basis is defined as the mass ratio of each product to all products. The mass balance is above 95 wt% for all catalytic tests in this study.

S1.4. Analysis of retained organics

The retained organics in the catalysts after MTO reaction were analyzed by GC-MS. The catalyst was dissolved in a hydrofluoric acid solution (40 wt%), and the retained organics were extracted with dichloromethane (CH_2Cl_2) and analyzed by an Agilent 7890B-GC equipped with an FID and a Agilent 5795C Mass Selective Detector with a HP-5 capillary column (30 m × 0.25 mm × 0.25 μm). The structures annotated onto the chromatograms are peak identifications reference to NIST database. The amount of retained organics was normalized with n-heptane as the internal standard.

Contents:

Figures

Scheme

Tables

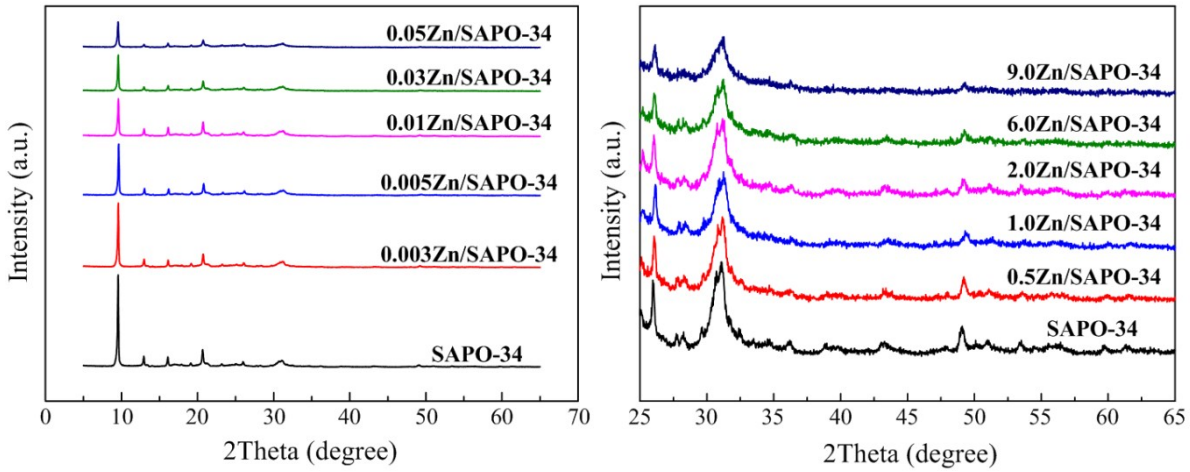

Fig. S1 XRD patterns of SAPO-34 and Zn/SAPO-34 zeolites

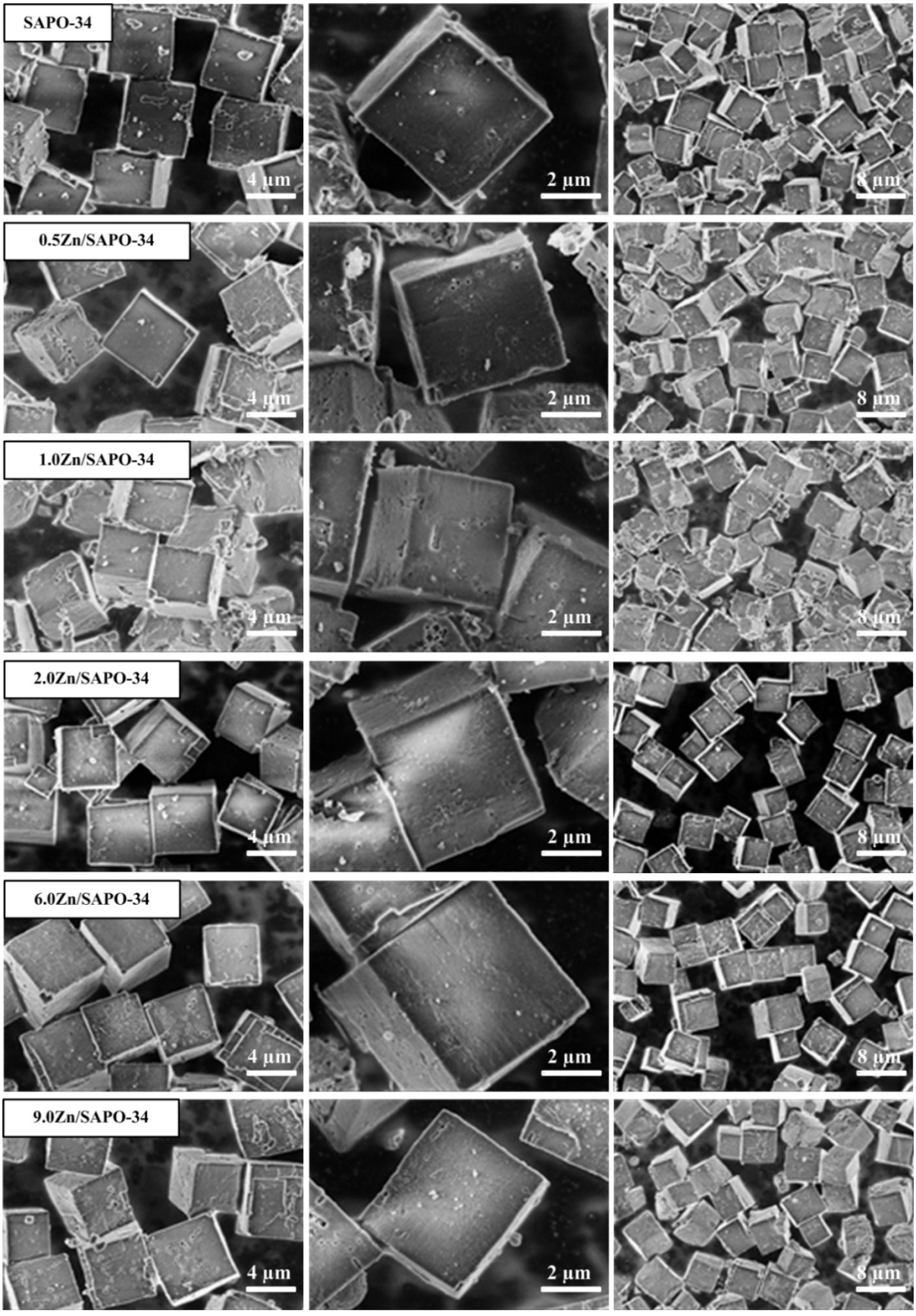

Fig. S2 SEM image of SAPO-34 and Zn/SAPO-34 zeolites

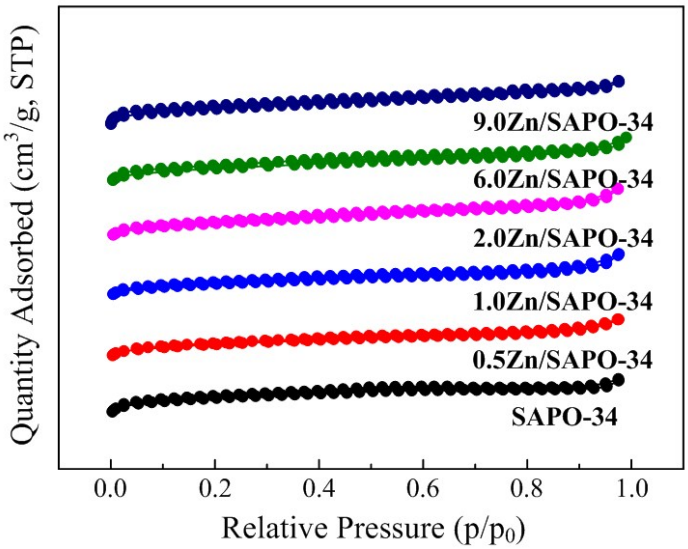

Fig. S3 Nitrogen adsorption-desorption isotherms of SAPO-34 and Zn/SAPO-34 zeolites

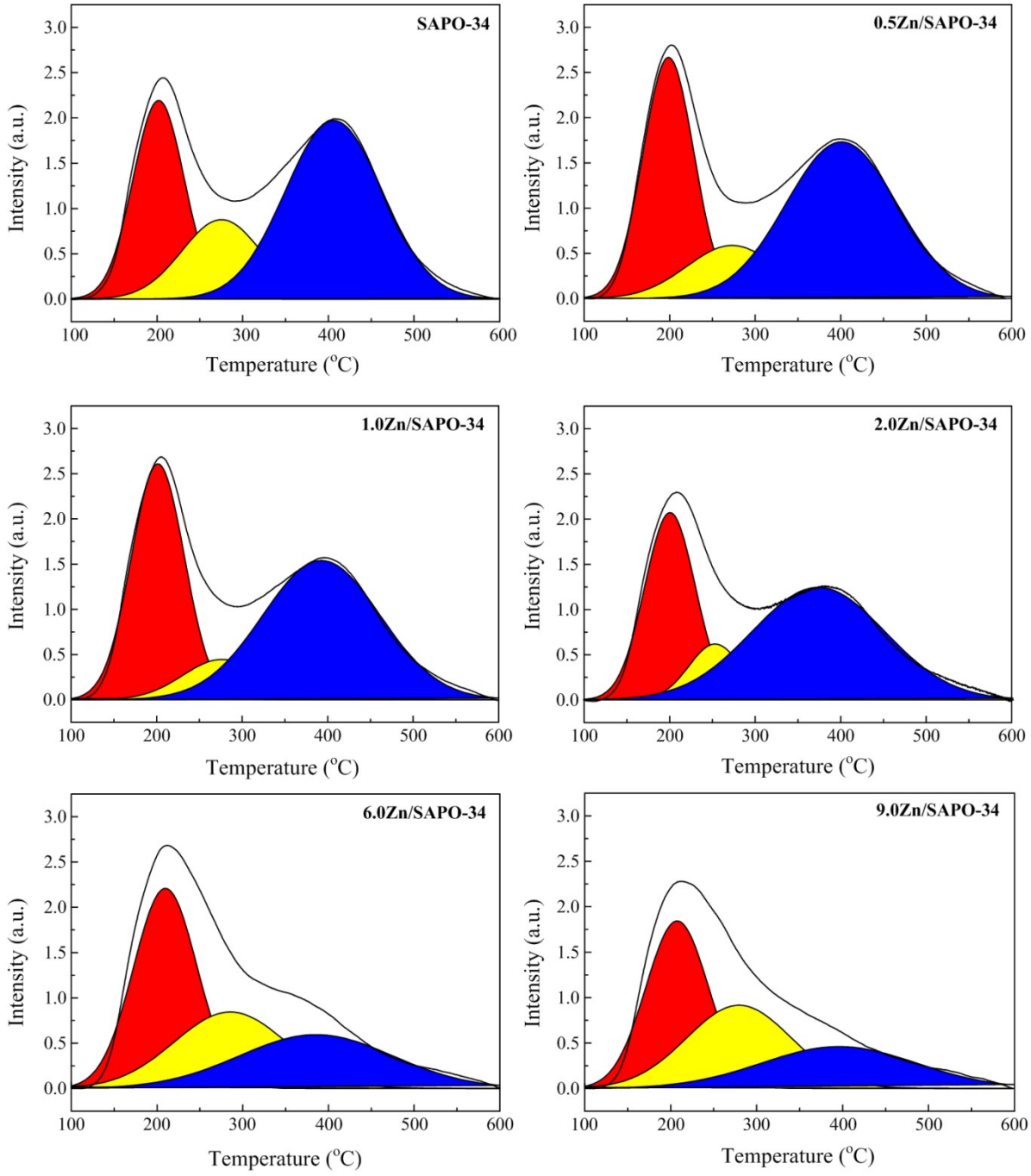

Fig. S4 NH_3-TPD profiles of SAPO-34 and Zn/SAPO-34 zeolites

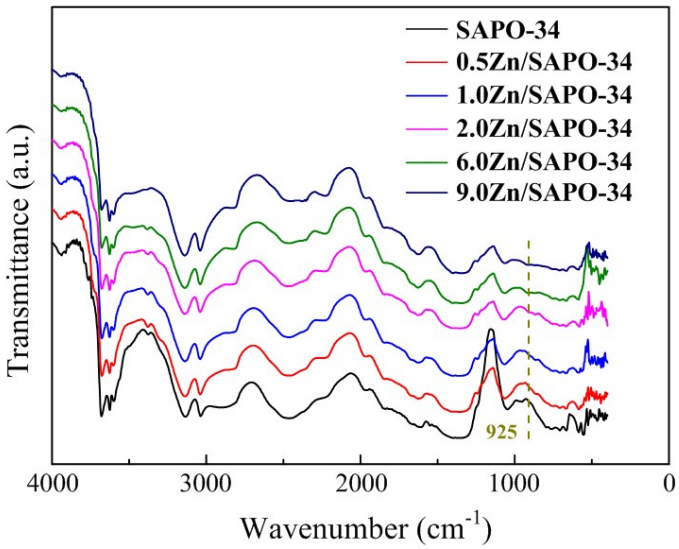

Fig. S5 FTIR spectra of SAPO-34 and Zn/SAPO-34 zeolites

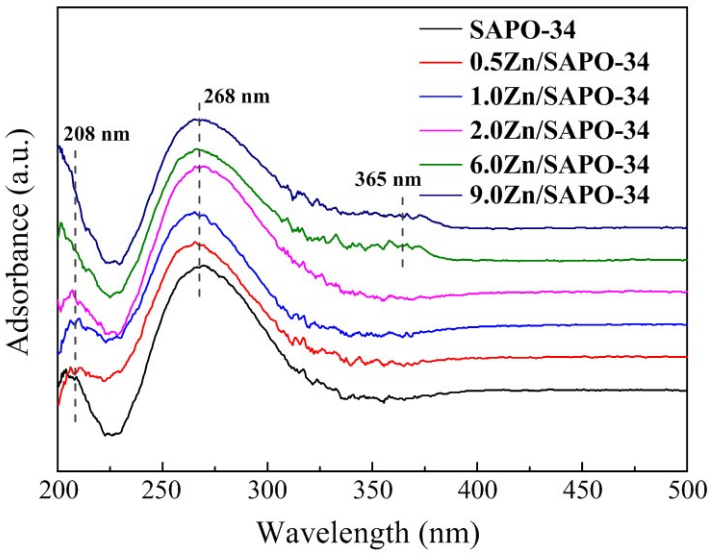

Fig. S6 UV-vis DRS spectra of SAPO-34 and Zn/SAPO-34 zeolites

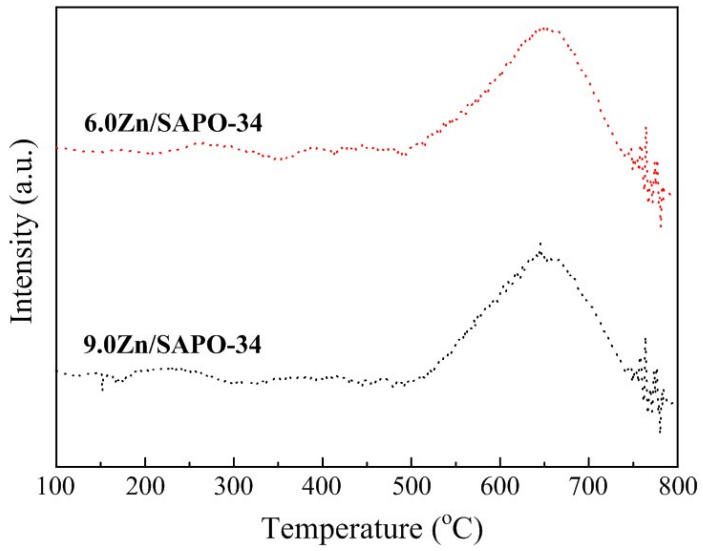

Fig. S7 H_2-TPR profiles of 6.0Zn/SAPO-34 and 9.0Zn/SAPO-34 zeolites

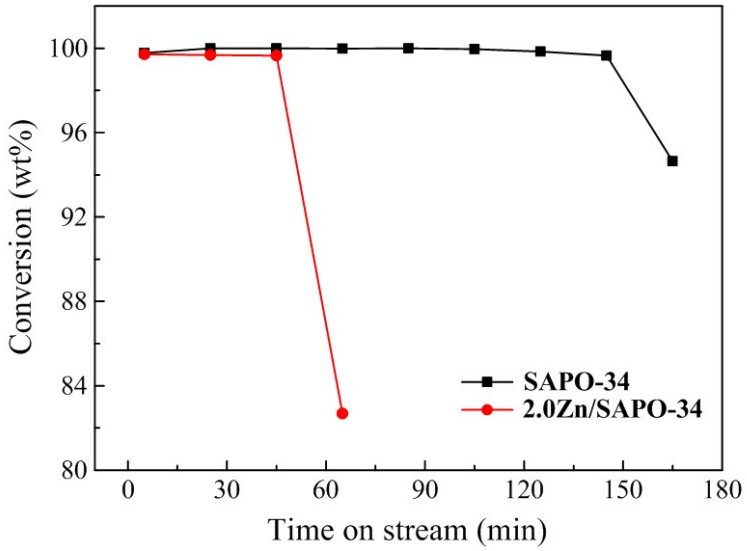

Fig. S8 Methanol conversion of SAPO-34 and 2.0Zn/SAPO-34 zeolites with time on stream

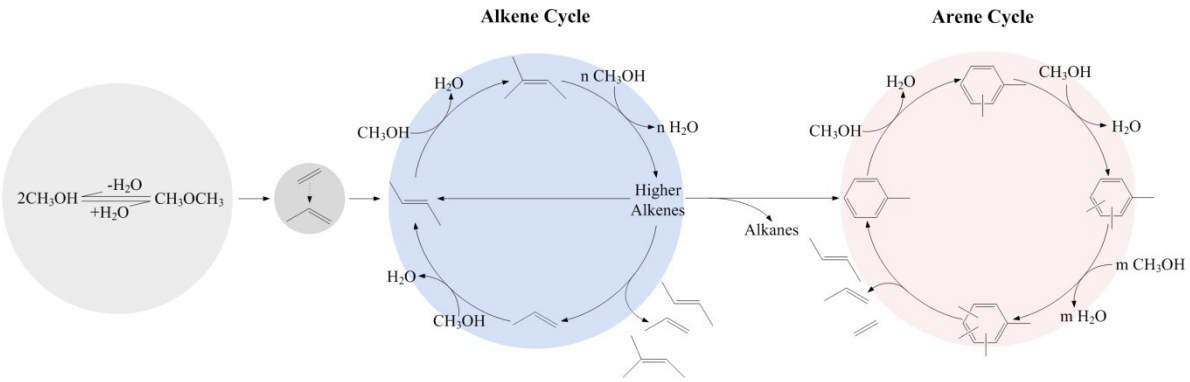

Scheme S1 Reaction pathway for methanol conversion

Table S1 Catalytic performance of SAPO-34 and Zn/SAPO-34 zeolites for methanol conversion

Sample	SAPO-34	0.5Zn/SAPO-34	1.0Zn/SAPO-34	2.0Zn/SAPO-34	6.0Zn/SAPO-34	9.0Zn/SAPO-34
Conversion (wt%)	99.93	99.85	99.83	99.24	97.30	90.65
Yield (wt%)						
H_2	0.14	0.15	0.28	0.70	1.84	2.04
CO_x	0.08	0.05	0.03	0.08	0.09	0.05
CH_4	1.50	1.95	2.75	2.92	4.20	4.72
C_2H_6	0.73	0.72	0.71	0.63	0.63	0.62
C_2H_4	18.51	20.80	22.40	23.58	23.20	22.58
C_3H_8	1.60	1.60	1.13	0.87	0.54	0.25
C_3H_6	16.57	14.88	13.54	12.59	10.76	9.60
C_4H_{10}	0.17	0.12	0.09	0.07	0.03	0.03
C_4H_8	4.06	2.95	2.72	2.44	2.25	1.50
C_5^+	0.40	0.11	0.04	-	-	-
C_2+C_3	35.08	35.68	35.94	36.17	33.96	32.18
C_2-$C_4^=$	39.14	38.63	38.66	38.61	36.21	33.68
$C_2^=/C_3^=$	1.12	1.40	1.66	1.87	2.16	2.35

Table S2 Catalytic performance of SAPO-34 and 2.0Zn/SAPO-34 zeolites for methanol conversion with time on stream

Sample	SAPO-34		2.0Zn/SAPO-34	
Time on stream (min)	0-5	30-35	0-5	30-35
Conversion (wt%)	99.93	80.37	99.24	75.12
Yield (wt%)				
H_2	0.14	0.06	0.70	0.24
CO_x	0.08	0.03	0.08	0.01
CH_4	1.50	2.61	2.92	3.09
C_2H_6	0.73	0.58	0.63	0.43
C_2H_4	18.51	14.75	23.58	16.55
C_3H_8	1.60	1.42	0.87	0.54
C_3H_6	16.57	11.69	12.59	9.16
C_4H_{10}	0.17	0.11	0.07	0.05
C_4H_8	4.06	3.12	2.44	2.41
C_5^+	0.40	0.49	-	0.40
C_2+C_3	35.08	26.44	36.17	25.71
$C_2-C_4^=$	39.14	29.56	38.61	28.12
$C_2^=/C_3^=$	1.12	1.26	1.87	1.81

Table S3 Acidity analysis of SAPO-34 and Zn/SAPO-34 zeolites

Sample	Acidity (mmol/g)			
	Weak	Medium	Strong	Total
SAPO-34	0.272	0.168	0.461	0.901
0.5Zn/SAPO-34	0.314	0.123	0.445	0.882
1.0Zn/SAPO-34	0.311	0.078	0.405	0.794
2.0Zn/SAPO-34	0.240	0.074	0.379	0.693
6.0Zn/SAPO-34	0.282	0.190	0.182	0.654
9.0Zn/SAPO-34	0.237	0.197	0.145	0.579

Table S4 Methanol conversion and product selectivity of SAPO-34 zeolite versus resident time in MTO reaction at 400 and 450 °C

T (°C)	R.T. (ms)	Con. (wt%)	Selectivity (C-%)							
			C_2H_4	C_3H_6	C_4H_8	CH_4	C_2H_6	C_3H_8	C_4H_{10}	C_5^+
400	25.7	66.4	30.17	44.57	14.17	0.91	0.46	5.49	0.91	1.14
	49.4	89.0	35.89	43.66	11.89	0.91	0.69	4.80	0.69	1.14
	69.6	93.2	36.57	43.66	11.66	1.14	0.69	4.11	0.69	0.69
	117.8	96.2	40.69	42.51	8.91	1.60	1.14	4.11	0.46	-
450	23.1	74.2	38.40	45.49	11.43	0.46	-	2.51	0.23	1.83
	46.7	88.2	40.23	43.66	10.06	1.60	0.69	2.29	-	1.37
	65.8	90.5	44.11	40.23	8.91	2.29	0.91	2.29	-	0.69
	119.8	98.3	44.11	37.94	6.40	2.51	1.14	2.06	-	0.23

Table S5 Summary of results of methanol conversion over SAPO-34 zeolites in this work and literatures

Zeolite	Conversion (wt%)	Selectivity (C-%)		E/P	Reaction conditions	Reference
		Ethene	Propene			
SAPO-34	99.9	42.3	37.9	1.12	500 °C, 10.02 h^{-1}, MeOH	This work
0.5Zn/SAPO-34	99.9	48.1	34.4	1.40		
1.0Zn/SAPO-34	99.8	51.7	31.2	1.66		
2.0Zn/SAPO-34	99.2	54.7	29.2	1.87		
6.0Zn/SAPO-34	97.3	55.7	25.8	2.16		
9.0Zn/SAPO-34	90.7	57.5	24.4	2.35		
SAPO-34	99.2	42.6	32.6	1.31	450 °C, 14.22 h^{-1}, MeOH	[1]
SAPO-34	98.5	47.0	34.7	1.35		
SAPO-34	100.0	31.0	39.0	0.79	475 °C, 2.0 h^{-1}, MeOH/H_2O = 40:60 (w)	[2]
Zn/SAPO-34	100.0	39.7	35.1	1.13		
SAPO-34	100.0	17.1	27.3	0.63	400 °C, 2.0 h^{-1}, MeOH	[3]
Hi-SAPO-34	100.0	22.0	28.4	0.77		
Hi-SAPO-34	100.0	26.8	30.1	0.89		
Hi-SAPO-34	100.0	25.0	30.0	0.83	400 °C, 4.0 h^{-1}, MeOH	[4]
SAPO-34	100.0	24.0	39.5	0.61	425 °C, 2.0 h^{-1}, MeOH/H_2O = 50:50 (mol)	[5]
Hi-Zn/SAPO-34	100.0	33.0	35.5	0.93		
SAPO-34	100.0	28.0	39.0	0.72	475 °C, 2.0 h^{-1}, MeOH/H_2O = 40:60 (w)	[6]
Zn/SAPO-34	100.0	35.0	40.0	0.88		
SAPO-34	100.0	33.2	40.7	0.82	450 °C, 2.0 h^{-1}, MeOH/H_2O = 40:60 (w)	[7]
SAPO-34	100.0	35.1	40.5	0.87		
SAPO-34	100.0	38.0	38.0	1.00	500 °C, 2.0 h^{-1}, MeOH	[8]
Zn/SAPO-34	100.0	44.0	34.0	1.30		
SAPO-34	100.0	64.0	20.0	3.20	500 °C, GHSV = 4200 $cm^3/g/h$ MeOH/H_2O = 30:70 (mol)	[9]
Fe/SAPO-34	100.0	7.5	1.0	7.50		
Ag/SAPO-34	100.0	67.0	12.0	5.58		
K/SAPO-34	100.0	69.0	21.0	3.29		

References

[1] T. Álvaro-Muñoz, C. Márquez-Álvarez and E. Sastre, Catal. Today, 2012, **179**, 27-34.

[2] J. Zhong, J. Han, Y. Wei, S. Xu, Y. He, Y. Zheng, M. Ye, X. Guo, C. Song and Z. Liu, Chem. Commun., 2018, **54**, 3146-3149.

[3] Q. Sun, N. Wang, D. Xi, M. Yang and J. Yu, Chem. Commun., 2014, **50**, 6502-6505.

[4] B. Yang, P. Zhao, J. Ma and R. Li, Chem. Phys. Lett., 2016, **665**, 59-63.

[5] C. Sun, Y. Wang, Z. Wang, H. Chen, X. Wang, H. Li, L. Sun, C. Fan, C. Wang and X. Zhang, Comptes Rendus Chim., 2018, 21, 61-70.

[6] J. Zhong, J. Han, Y. Wei, S. Xu, T. Sun, X. Guo, C. Song and Z. Liu, J. Energy Chem., 2018.

[7] G. Liu, P. Tian, Q. Xia and Z. Liu, J. Nat. Gas Chem., 2012, **21**, 431-434.

[8] J. Zhong, J. Han, Y. Wei, S. Xu, T. Sun, X. Guo, C. Song and Z. Liu, Chin. J. Catal., 2018, **39**, 1821-1831.

[9] K. Mirza, M. Ghadiri, M. Haghighi and A. Afghan, Microporous Mesoporous Mater., 2018, **260**, 155-165.